ACS OMEGA

Open Access

http://pubs.acs.org/journal/acsodf

Article

Influence Mechanism of Gas Pressure on Multiscale Dynamic Apparent Diffusion-Permeability of Coalbed Methane

Zhiqiang Li, Aijie Wang, Lin Li,* Junliang Li, Ningchao Zhang, Kaiqi Jin, and Ju Chang

Cite This: *ACS Omega* 2023, 8, 35964−35974

Read Online

ACCESS | Metrics & More | Article Recommendations

ABSTRACT: The permeability and diffusion coefficient of coal show multiscale characteristics due to the influence of multiscale pore sizes. The gas pressure will continuously decrease during the coalbed methane (CBM) extraction. However, there are contradictory perceptions in the effect of gas pressure on the diffusion coefficient and permeability. Therefore, it is essential to clarify the influence mechanism of gas pressure on multiscale diffusion-seepage. Diffusion-seepage experiments are carried out using particle coal and cylindrical coal without stress loading. Meanwhile, seepage experiments measured by the steady-state method are conducted under stress loading. The results show that the apparent diffusion coefficient is dynamically attenuated with time in the experiments of particle and cylindrical coal. A new model of multiscale dynamic apparent diffusion is proposed. The mechanism of gas flow in multiscale pores is elucidated. The multiscale pores determine the attenuation of the diffusivity and permeability of coal. The initial apparent permeability decreases and then increases with the increase of gas pressure, which is caused by the effect of gas pressure stretching and multiscale flow regime. Three patterns of permeability with gas pressure, monotonically increasing, monotonically decreasing, and U-shaped changes, will occur.

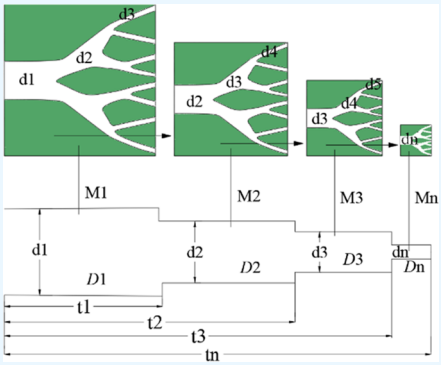

1. INTRODUCTION

Coalbed methane (CBM) is a clean and unconventional gas energy. The development of CBM is beneficial to the energy supply, environmental protection, and mining safety. CBM extraction has become a significant national demand in major coal-mining countries, such as the United States, Australia, and China.[1−5] However, the low permeability of coal severely restricts the efficiency of CBM exploitation. The rapid attenuation of the gas flow rate and production occurs in the initial period of CBM extraction. The reasons for this phenomenon are not known. Coalbed methane extraction is a continuous process of pressure reduction, seepage, diffusion, and desorption. The influence of gas pressure reduction on seepage and diffusion has attracted attention in the industry. It is significant to investigate the impact mechanism of gas pressure on the permeability and diffusivity of coal.

The diffusion coefficient and permeability are the most critical parameters that affect the CBM flow. The effects of gas pressure on diffusion coefficient still show different experimental results and interpretations. (1) The diffusion coefficient increases monotonically with the increase of gas pressure.[6−10] (2) The diffusion coefficient decreases monotonically with the gas pressure increasing.[11−17] (3) The diffusion coefficient decreases and then increases as the gas pressure increases.[18−20] (4) The diffusion coefficient fluctuates irregularly with increasing gas pressure.[21−24] It is noted that a particle coal was used to measure the diffusion coefficient in most of the diffusion experiments. The basic assumption is that particle coal can be approximated as a coal matrix, in which the gas flow belongs to diffusion driven by concentration. The model used for the calculation is the spherical diffusion model.

However, the experiments and models of particle coal can only reflect the diffusion process of gas flow in a coal matrix. The conventional seepage experiments measured by the steady-state method cannot reflect the diffusion process. The two types of experiments are not unified in terms of experimental principles, measurement methods, and flow mechanisms and cannot especially reflect the continuous seepage-diffusion process of large-scale raw coal. Therefore, the relationship between the gas pressure and the diffusion coefficient and permeability of coal cannot be simultaneously interpreted.

There are a large number of multiscale pores in coal that greatly affect the diffusion coefficient and permeability of the coal. The study in literature[25] showed that the effective diffusion coefficient decreases by millions of times with time even without stress loading. During the process of coalbed methane production, a shift in the flow regimes will occur due

Received: May 30, 2023
Accepted: September 7, 2023
Published: September 23, 2023

to a dramatic decrease in gas pressure and pore size. The impact mechanism of gas pressure on the multiscale diffusion coefficient and permeability is an important scientific issue.

To solve the problems above, in this paper, the experiments of continuous diffusion-seepage are performed under different pore pressures using particle and cylindrical coal. A novel multiscale model of dynamic apparent diffusion is proposed. The impact mechanism of gas expansion and flow regimes on apparent diffusion-permeability is interpreted, which unifies the previous contradictory understanding. The study provides a new viewpoint for understanding the rapid attenuation of the production of low-permeability coalbed methane.

2. EXPERIMENTS OF DIFFUSION-SEEPAGE AND STEADY-STATE SEEPAGE OF GAS

2.1. Experimental Methods and Apparatus. *2.1.1. Coal Sample Preparation.* The coal samples are collected from the Duanshi coal mine in China, and the ϕ 50 mm × 100 mm cylindrical coal are drilled axially along the seam, and some of the coal is crushed into 0.18−0.25 mm coal particles. All coal samples are vacuumed and dried in a drying oven at 80 °C without oxygen to remove moisture. The results of the basic parameters of the coal samples are shown in Table 1.

Table 1. Basic Parameters of Coal Samples

parameters	values
moisture (%)	1.08
ash (%)	10.17
volatile matter (%)	8.90
density (g/cm^3)	1.59
porosity (%)	5.25
a_{tw} (adsorption constant) (cm^3/g)	43.49
b_{tw} (adsorption constant) (MPa^{-1})	1.03

2.1.2. Experiments of Diffusion-Seepage of Gas for Cylindrical and Particle Coal. The experiments of gas diffusion-seepage with cylindrical coal and particle coal without stress loading are conducted, respectively. As shown in Figure 1, valves V3, V4, and V8 are closed, valves V1, V2, and V5 are opened, the methane cylinder is turned on, pressure-regulating valve 1 is controlled, and the gas pressure is set to 3 MPa to inflate the cylindrical coal sample in the diffusion-seepage device of cylindrical coal. After the cylindrical coal sample reaches adsorption equilibrium for 72 h, V1, V2, and V5 and pressure-regulating valves 1 are closed. Valve V8 is opened, and gas in the cylindrical coal is released. After 5 s, valve V9 is connected to measure the gas flowing from the cylindrical coal for 180 min, and the accumulative desorption volume of gas is measured by the measuring cylinder1 in the water sink using the drainage method. When the cumulative gas volume is large and the volume of cylinder1 is not sufficient to determine the entire cumulative volume, it is necessary to switch to the measuring cylinder234 to determine the remaining cumulative desorption volume.

The accumulative desorption volume is recorded every 30 s until the desorption volume changes very little and the test is finished. The gas pressure is changed to 3, 2, 1, and 0.5 MPa in turn, and the above experimental operations are repeated to complete the diffusion-seepage experiments of gas flow in cylindrical coal.

The experiments of diffusion-seepage of gas flow in particle coal are similar to those of cylindrical coal. The diffusion-seepage apparatus of particle coal is opened, the gas pressure is changed to 3.5 2.5, 1, and 0.5 MPa in turn, and the above operations are repeated to complete the diffusion-seepage testing of gas flow in granular coal without stress loading.

2.1.3. Steady-State Permeability Experiments of Gas Flow in Cylindrical Coal. As shown in Figure 2, a cylindrical coal is placed into the triaxial seepage device, and the axial pressure of 8 MPa and the confining pressure of 4 MPa are kept. Valves V3 and V4 are closed, valves V1, V2, V5 are turned on, and solenoid flow valve (meter) F1 is opened. The upstream pressure (pressure gauge 1 and 2) is kept at 3 MPa by regulating pressure valve 1. The outlet flow rate of gas is monitored by solenoid flow meter F1, and the permeability is determined after the flow rate is stable. The gas pressures are changed to 3, 2, 1, and 0.5 MPa in turn, and the above operations are repeated to measure the steady-state permeability at different gas pressures.

2.2. Data Processing. After the diffusion-seepage experiment, the accumulated volume of gas diffusion is converted into the diffusion quantity Q_t per unit mass of coal under standard conditions. Divided by the ultimate diffusion quantity, Q_∞, a diffusion ratio curve versus time, $Q_t/Q_\infty \sim t$, is obtained. Owing to the drainage method is used to measure

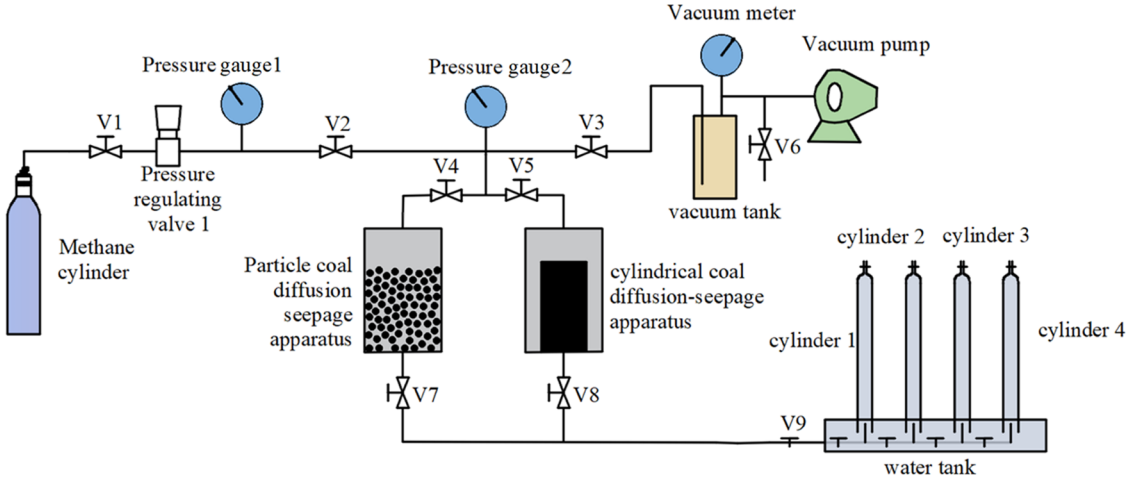

Figure 1. Experimental system of diffusion-seepage for particle and cylindrical coal.

https://doi.org/10.1021/acsomega.3c03806
ACS Omega 2023, 8, 35964−35974

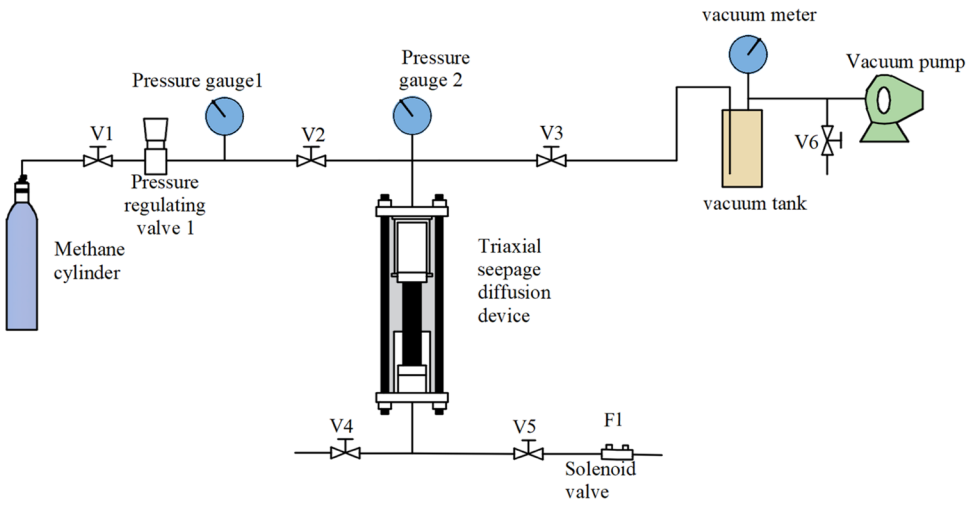

Figure 2. Experimental system of steady-state permeability for cylindrical coal.

the gas diffusion, the ultimate diffusion quantity Q_∞ is equal to the difference that initial gas content, Q, minus gas content, Q_a, at atmospheric pressure, that is, $Q_\infty = Q - Q_a$, Q, Q_a under experimental conditions are calculated according to the following equation

$$Q = \frac{a_{tw} b_{tw} p}{1 + bp}(1 - A_{ad}) + \frac{10p\phi \cdot 273}{\rho(273 + \theta_w)} \quad (1)$$

where: a_{tw}, b_{tw} are the adsorption constant; p is the adsorption equilibrium pressure; A_{ad} is ash; θ_w is the experimental temperature; ρ is the coal density; ϕ is the coal porosity; Q is the total gas content corresponding to the initial adsorption equilibrium pressure p, and Q_a is the gas content at atmospheric pressure. When calculating the gas content Q_a at atmospheric pressure, the pressure p in eq 1 is replaced with atmospheric pressure.

3. ANALYSIS OF DIFFUSION-SEEPAGE EXPERIMENTS USING CLASSICAL DIFFUSION MODEL

3.1. Comparison of Classical Diffusion Model and Experiments for Particles Coal. The analytical solution of the classical model of spherical diffusion can be expressed by the following formula.[26]

$$\frac{Q_t}{Q_\infty} = 1 - \frac{6}{\pi^2}\sum_{n=1}^{\infty}\frac{1}{n^2}\exp\left(-\frac{n^2\pi^2 D}{r_0^2}t\right) \quad (2)$$

where Q_t is the accumulative diffusion volume at time t, cm^3/g; Q_∞ is the ultimate diffusion volume, cm^3/g; Q_t/Q_∞ is the diffusion ratio at time t; D is the apparent diffusion coefficient, cm^2/s; r_0 is the radius of coal particle, cm.

To simplify the calculation, eq 3 can be obtained when taking $n = 1$ in eq 2. This treatment can clearly demonstrate the change of the constant diffusion coefficient with time.

$$\ln\left(1 - \frac{Q_t}{Q_\infty}\right) = -\lambda t + A$$

$$\lambda = \frac{\pi^2 D}{r_0^2},\ A = \ln\frac{6}{\pi^2} \quad (3)$$

The experimental data of 2.5 MPa are selected, and the experimental and theoretical curves of $\ln(1 - Q_t/Q_\infty) \sim t$ are plotted in Figure 3a according to eq 3 and that of $Q_t/Q_\infty \sim t$ are plotted in Figure 3b according to eq 2.

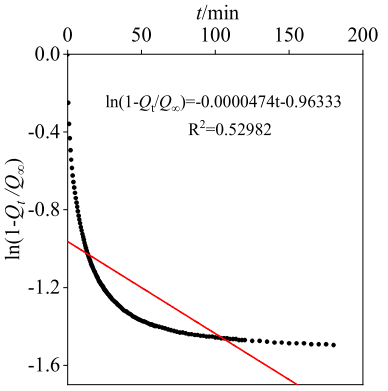

(a) Diffusion parameter fitting

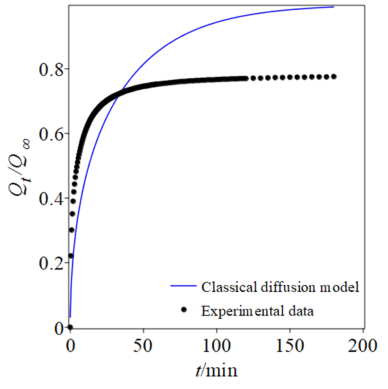

(b) Comparison between diffusion experiment and classical apparent model.

Figure 3. Comparison of diffusion parameter fitting and classical models for 2.5 MPa gas pressure granular coal.

As shown in Figure 3a, the experimental curve of $\ln(1 - Q_t/Q_\infty) \sim t$ attenuates dynamically with time, and its tangent slope decreases with time. r_0 and π in eq 3 are the known constants, which indicates that the apparent diffusion coefficient D should be a variable that attenuates with time. However, in the classical diffusion model of eq 3, the apparent

https://doi.org/10.1021/acsomega.3c03806
ACS Omega 2023, 8, 35964−35974

diffusion coefficient, D, is a constant, which leads to the inconsistency between the experiment and theory as the straight line is shown in Figure 3a.

Substituting $\lambda = 0.0000474$ in Figure 3a into eq 2, a comparison of the theoretical and experimental curves for CH_4 at 2.5 MPa of gas pressure is obtained as shown in Figure 3b. Figure 3b shows that the experiment value of diffusion ratio Q_t/Q_∞ is larger than the theoretical value of the classical diffusion model in 0−31 min; however, the experimental value is smaller than the theoretical value after 31 min. In the late stage of diffusion, the errors between the experimental value and classical diffusion model gradually increase and the two curves deviate seriously in the late stage. The classical diffusion model cannot accurately describe the full-time process of gas diffusion. The defect of classical diffusion mode lies in the assumption that the apparent diffusion coefficient is constant, which contradicts with the experimental diffusion coefficient decaying with time.

3.2. Comparison of Classical Diffusion Models and Experiments for Cylindrical Coal. The analytical solution of the classical model of radial diffusion is shown in eq 4[26]

$$\frac{Q_t}{Q_\infty} = 1 - 4\sum_{n=1}^{\infty}\frac{\exp(-a_n^2 Dt)}{a_n^2 R^2} \tag{4}$$

where Q_t is the accumulative diffusion volume at time t, cm^3/g; Q_∞ is the ultimate diffusion volume, cm^3/g; Q_t/Q_∞ is the diffusion ratio at time t; D is the apparent diffusion coefficient, cm^2/s; a_nR is the n-th positive root of zero-order Bessel function of the first kind $J_0(a_nR) = 0$; R is the radius of cylindrical coal, cm.

In eq 4, when $n > 1$, it is difficult to solve the apparent diffusion coefficient D. The same treatment as eq 3 is used to simplify eq 4 by taking $n = 1$.

$$\ln\left(1 - \frac{Q_t}{Q_\infty}\right) = -\omega t + B$$
$$\omega = a_1^2 D,\ B = \ln\frac{4}{a_1^2 R^2} \tag{5}$$

where a_1R is the first positive root of the zero-order Bessel function of the first kind $J_0(a_nR) = 0$. The experimental data of the cylindrical coal are processed according to eq 5, and the experimental data of 2 MPa are selected to plot the curve of $\ln(1 - Q_t/Q_\infty) \sim t$ shown in Figure 4a. The experimental and theoretical curves are plotted in Figure 4b according to eq 4.

Figure 4a shows that the experimental curve of $\ln(1 - Q_t/Q_\infty) \sim t$ for cylindrical coal decreases dynamically with time and its tangent slope decreases with time. a_1 and R in eq 5 are the known constants, which demonstrates that the apparent diffusion coefficient D is a variable changing with time. Substituting the fitted value $\omega = 0.00227$ in Figure 4a into eq 4, a comparison of the theoretical and the experimental curve at 2.0 MPa of gas pressure is obtained in Figure 4b. Figure 4b shows that the classical diffusion model of eq 4 cannot accurately describe the full-time process of the gas flow. The main reason for the errors is the same as the model of eq 2 for the particle coal, which assumes that the apparent diffusion coefficient is a constant.

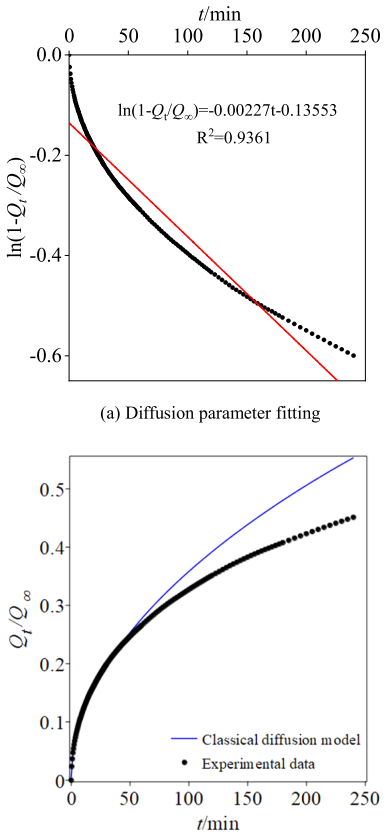

Figure 4. Comparison of diffusion parameter fitting and classical models for 2.0 MPa gas pressure cylindrical coal.

4. MODEL AND MECHANISM OF MULTISCALE DYNAMIC DIFFUSION-SEEPAGE

4.1. Model of Multiscale Dynamic Apparent Diffusion-Seepage for Particle Coal. The apparent diffusion coefficient is related to the pore structure of coal. The experiments of gas diffusion-seepage in a coal particle show that the apparent diffusion coefficient attenuates with time. The apparent diffusion coefficients in the previous experiments with time include the processes of seepage and diffusion simultaneously. The corresponding model should be called the model of dynamic apparent diffusion-seepage.

To accurately describe the dynamic attenuation of the apparent diffusion coefficient, a negative exponential function is proposed to present the variation of the apparent diffusion coefficient.[27] Furthermore, we find that the conversion relationship between the dynamic apparent diffusion coefficient $D(t)$ and the constant diffusion coefficient D is as follows.

$$\begin{cases} D(t) = D_0\exp(-\beta t) \\ D\cdot t = \int_0^t D(t)\mathrm{d}t \\ \quad = \dfrac{D_0}{\beta}(1 - \exp(-\beta t)) \end{cases} \tag{6}$$

where $D(t)$ is the dynamic apparent diffusion coefficient that decays with time, cm^2/s; D_0 is the initial apparent diffusion coefficient when $t = 0+$, cm^2/s; β is the attenuation coefficient

https://doi.org/10.1021/acsomega.3c03806
ACS Omega 2023, 8, 35964−35974

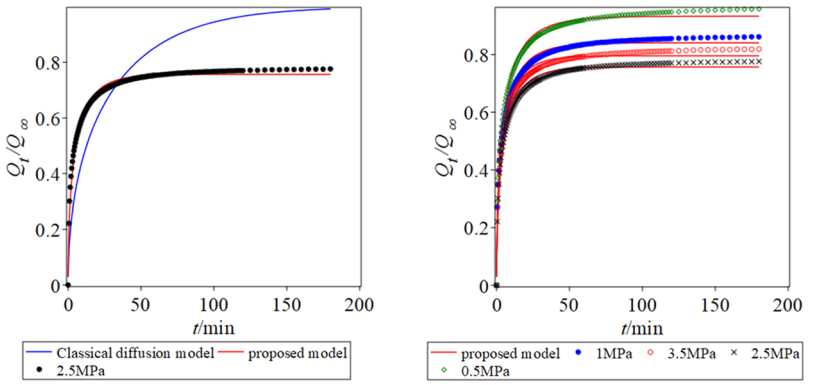

(a) Comparison between classical diffusion model and the model of dynamic apparent diffusion-seepage at 2.5MPa of gas pressure for CH_4.

(b) Fitting of CH_4 experiment by the model of dynamic apparent diffusion-seepage.

Figure 5. Dynamic apparent diffusion-percolation model analysis of granular coal.

of the dynamic apparent diffusion coefficient, s^{-1}, which reflects the degree of transition from the exterior large pore to the interior small pore at different scales; and t is the time, s.

The basic assumptions of the apparent diffusion-seepage process are (1) coal grains are isotropic spheres; (2) the pore structure of coal grains consists of multiscale inhomogeneous pores, and the apparent diffusion coefficient attenuates dynamically with the extension of time.

According to the assumptions above and the classical diffusion model, a model of multiscale dynamic diffusion-seepage is established, as shown in eq 7.

$$\begin{cases} \dfrac{\partial C}{\partial t} = D(t)\left(\dfrac{\partial C^2}{\partial r^2} + \dfrac{2}{r}\dfrac{\partial C}{\partial r}\right) \\ \dfrac{\partial C}{\partial r} = 0 \ (r = 0, \ t > 0) \\ C = C_0 \ (t = 0, \ 0 \le r \le r_0) \\ C = C_1 \ (t > 0, \ r = r_0) \end{cases} \tag{7}$$

where C is the methane mass concentration, g/cm^3; r is the diffusion path, cm; C_0 is the methane mass concentration at the initial adsorption equilibrium, g/cm^3; C_1 is the mass concentration of methane at the surface of coal grain, g/cm^3; r_0 is the radius of the grain coal, cm.

Substituting eq 6 into eq 7 and solving it by the separation of variables method,[22] we get

$$\frac{Q_t}{Q_\infty} = 1 - \frac{6}{\pi^2} \sum_{n=1}^{\infty} \exp\left[-\frac{n^2\pi^2 D_0}{r_0^{\,2}\beta}(1 - \exp(-\beta t))\right] \tag{8}$$

4.2. Model Verification for Particle Coal. The experimental data of particle coal at 2 MPa of pressure are processed according to eq 2 and eq 8, respectively. The comparison of fitting between the model of dynamic diffusion-seepage and the classical model is shown in Figure 5a,5b.

Figure 5a shows that compared with the classical diffusion model, the model of dynamic apparent diffusion-seepage can accurately describe the full-time flow process for CH_4. As shown in Figure 5b, the model of dynamic diffusion-seepage is validated at other pressures, such as 0.5 1, 2.5, and 3.5 MPa.

4.3. Model of Multiscale Dynamic Apparent Diffusion-Seepage for Cylindrical Coal. Similar to the treatment of the model of dynamic diffusion-seepage for particle coal, the negative exponential function of eq 6 is used to represent the variation of the apparent diffusion coefficient with time.

To accurately describe the full-time diffusion process of cylindrical coal, the assumptions of the model should be obeyed: (1) The radial dimension of cylindrical coal is smaller than the axial dimension, and the gas mainly flows out of the radial direction of coal. (2) The cylindrical coal is assumed to be heterogeneous, and the apparent diffusion coefficient of cylindrical coal varies dynamically with time, and the dynamic apparent diffusion coefficient includes both seepage and diffusion. (3) The gas flow process is a continuous process of diffusion-seepage and follows the law of mass conservation.

Based on the assumptions above, we obtain eq 9

$$\begin{cases} \dfrac{\partial C}{\partial t} = D(t)\left(\dfrac{\partial C^2}{\partial r^2} + \dfrac{1}{r}\dfrac{\partial C}{\partial r}\right) \\ \dfrac{\partial C}{\partial r} = 0 \ (r = 0, \ t > 0) \\ C = C_0 \ (t = 0, \ 0 \le r \le R) \\ C = C_a \ (r = R, \ t > 0) \end{cases} \tag{9}$$

where C is the methane diffusion mass concentration as a function of diffusion path r and time t, that is, $C = C(r, t)$, g/cm^3; r is the diffusion path, cm; C_0 is the methane mass concentration at the initial adsorption equilibrium, g/cm^3; C_a is the methane mass concentration on the surface of the cylindrical coal, g/cm^3; R is the radius of the cylindrical coal, cm.

Making a variable substitution and solving it by the separation of variables method, we get

$$\frac{M_t}{M_\infty} = \frac{Q_t}{Q_\infty} = 1 - \frac{4}{R^2} \sum_{n=1}^{\infty} \frac{\exp\left(a_n^{\,2}\frac{D_0}{\beta}(\exp(-\beta t) - 1)\right)}{a_n^{\,2}} \tag{10}$$

https://doi.org/10.1021/acsomega.3c03806
ACS Omega 2023, 8, 35964−35974

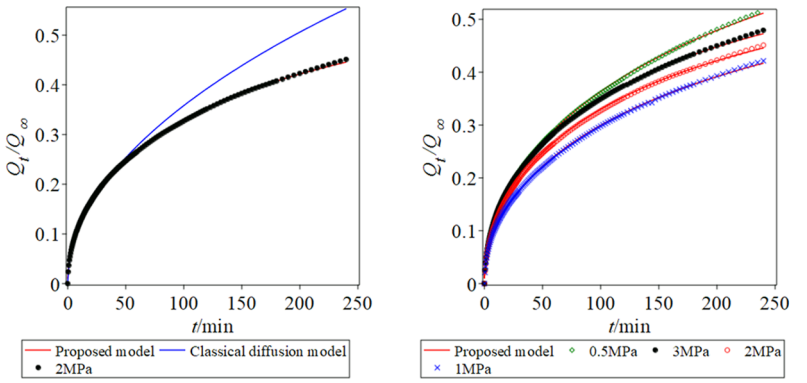

(a) Comparison of classical diffusion model and model of dynamic apparent diffusion-seepage with experiment at 2MPa of gas pressure.

(b) Comparison between model of dynamic apparent diffusion-seepage and experiments at different gas pressures.

Figure 6. Dynamic apparent diffusion-percolation model analysis of cylindrical coal.

4.4. Model Verification for Cylindrical Coal. The experimental data of diffusion-seepage of cylindrical coal are processed using eq 4 and eq 10, respectively. The comparison of the classical diffusion model and model of dynamic apparent diffusion-seepage with experiments for CH_4 is shown in Figure 6a and Figure 6b, respectively.

Figure 6a shows that the classical diffusion model of eq 4 cannot accurately describe the full-time process of gas diffusion and greatly deviates from the experimental data at a later stage. Compared with the classical model, the model of dynamic apparent diffusion-seepage, eq 10, has better computational accuracy. Furthermore, Figure 6b shows that the new proposed model has good agreement with the experimental data at different gas pressures.

4.5. Dynamic Diffusion-Seepage Mechanism of Gas Flow in Multiscale Pores. The attenuation of the apparent dynamic diffusion coefficient with time reflects the narrowing of the pore sizes during gas flowing in coal. There are multiscale pores in coal that are continuously distributed in a self-similar pattern. Accordingly, as shown in Figure 7, a multiscale pore structure diagram of coal is hypothesized. Figure 7 is a conceptualized model that is morphologically consistent with the fractal model of aperture in coal. The proposed model helps to better understand the multiscale permeability pattern of coal. In Figure 7, M1 represents an arbitrary size of coal block and M2 is the second-level coal matrix in M1. This rule applies to M3···M*n* and so on. d1, d2, d3···represent the diameters of multiscale pores, D1, D2, D3··· D*n* are the corresponding diffusion coefficients, and t1, t2, t3··· t*n* is time during gas flowing through the multiscale apertures.

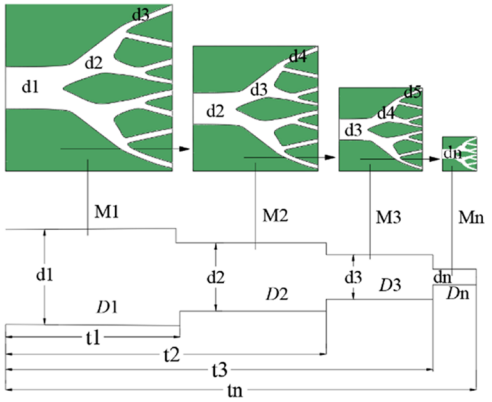

Figure 7. Schematic diagram of multiscale aperture structure.

In the initial stage during the time of t1, gas flows out of the large pore d1 in the coal block of M1 first. Due to the pore diameter of d1 is the largest, the flow resistance is the smallest, which causes the apparent diffusion coefficient D1 is the largest. During the time of t2, gas flows out of the smaller pore of d2 in the second-level coal matrix of M2. Owing to the decreases of pore diameter of d2, the flow resistance increases and the apparent diffusion coefficient D2 decreases. The law also applies to multiscale apertures from the third to n-th level. As time goes on, the flow process is influenced by the multiscale pores from the surface to the inside of coal. As shown in the lower part of Figure 7, the pore diameters from left to right gradually decreases, and the apparent diffusion coefficient at all levels gradually attenuates with time.

Due to the continuity of the pore structure in coal, the apparent diffusion coefficients of multiscale pores are dynamically connected in series by that of the single-level pore. As illustrated in Figure 7, the multiscale apparent diffusion coefficient is the series connection of D1 and D2 when the gas flows out from d2 of the M2 matrix to d1 of the M1 block. As the time goes by, gas flow through more and more pores connected in a series, causing the equivalent pore sizes connected in a series decrease gradually with the increase of time and levels. Accordingly, the apparent diffusion coefficient attenuates dynamically with time, which reflects the multiscale structure of coal pores.

5. EVOLUTION MECHANISM OF GAS PRESSURE ON MULTISCALE DYNAMIC APPARENT DIFFUSION-PERMEABILITY

5.1. Conversion of Dynamic Apparent Diffusion Coefficient to Apparent Permeability. In the experiments of diffusion-seepage of gas, the processes of gas flow include both diffusion and percolation, which cannot be distinguished. Based on the principle of mass conservation, the diffusion coefficient and permeability are apparently interconvertible in terms of mathematical meaning and experimental meaning.[27]

According to the ideal gas equation and Darcy law, we get the relationship between the dynamic apparent diffusion coefficient and apparent dynamic permeability can be determined as eq 11

https://doi.org/10.1021/acsomega.3c03806
ACS Omega 2023, 8, 35964−35974

$$k = \frac{\mu}{p}D \Rightarrow k(t) = \frac{\mu}{p}D(t) \tag{11}$$

where μ is the viscosity of gas, Pa·s; p is the gas pressure, MPa.

5.2. Multiscale Permeability Model Considering Gas Pressure, Stress, and Flow Regime. Gas presents different flow regimes when flowing through multiscale micro- and nanopores. The multiscale regimes are divided by Knudsen number (Kn) for gas flow in micro- and nanopores.[28] In Kn < 0.001, the flow regime is defined as a continuous flow, in which the slip effect on the boundary of the pore wall can be ignored. Darcy law is applicable in this regime. In 0.001 < Kn < 0.1, the flow regime is defined as slip flow, in which the slip effect on the boundary of the pore wall should be considered. In the range of 0.1 < Kn < 10, the regime is defined as transition flow, in which the slip effect on the pore wall becomes more pronounced. For Kn > 10, the regime is defined as a free molecular flow that can be described by Knudsen diffusion.

As shown in Figure 8, a diagram of flow regimes varying with multiscale pore sizes of coal in series is hypothesized.

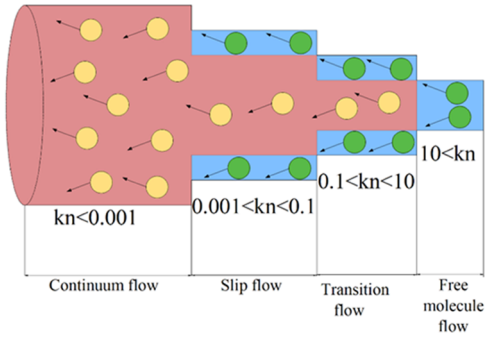

Figure 8. Diagram of flow regimes in multiscale series connection pores.

From left to right in Figure 8, at a low Knudsen number (Kn < 0.001), continuum flow occurs in large pores where the slip effect can be ignored. The red area represents the continuum flow in which yellow dots are the gas molecules colliding with each other. As the aperture decreases, the slip effect gradually appears in the second-level pore where slip flow occurs in the range of 0.001 < Kn < 0.1 The blue area represents the Knudsen diffusion layer where the gas molecules (green dots) mainly collide with the pore wall. As the aperture continues to reduce, the flow regime switches from slip flow to transitional flow at 0.1 < Kn < 10. In nanopores, the transport behavior of gas turns to free molecule flow at a high Knudesn number (Kn > 10), where the gas molecules completely collide with the pore wall.

Gas flow in micro- and nanopores is slow, and the microscopic mechanism is more complex and challenging to observe, so the transport coefficient is generally converted into apparent permeability to describe and analyze the gas flow regime in micro- and nanopores from a macroscopic point of view. Karniadakis established an expression for apparent permeability that can explain all flow regimes based on the Kn number and the dilution effect coefficient $\alpha(Kn)$.[29]

Due to the observation challenge of the gas flow in micro- and nanopores, an apparent permeability is adopted to analyze the gas flow regimes by combining Knudsen number with pore size. Karniadakis established an expression for apparent permeability that can describe the complete flow regimes, which is given by

$$\begin{cases} Kn = \dfrac{\lambda}{l}\lambda = \dfrac{K_B T}{\sqrt{2}\,\pi\varepsilon^2 p} \\ k_{\infty 0} = \dfrac{l^2}{8} \\ \alpha(Kn) = \dfrac{128}{15\pi^2}\tan^{-1}[4Kn^{0.4}] \end{cases} \tag{12}$$

where λ is the mean free path of gas molecules; l is the characteristic length of the pore and equals to the pore diameter; K_B is Boltzmann constant, 1.38 × 10^{-23}J/K; T is Kelvin temperature; ε is the molecular collision diameter; p is the gas pressure; Kn is the Knudsen number; $\alpha(Kn)$ is the dimensionless rarefaction effect coefficient.

Multiscale apparent permeability considering the flow regimes can be expressed as

$$k_{app} = k_{\infty 0}[1 + \alpha(Kn)Kn]\left[1 + \frac{4Kn}{1 + Kn}\right] \tag{13}$$

Based on eq 13, a model of multiscale apparent permeability considering the effects of stress, gas pressure, and flow regimes is established as

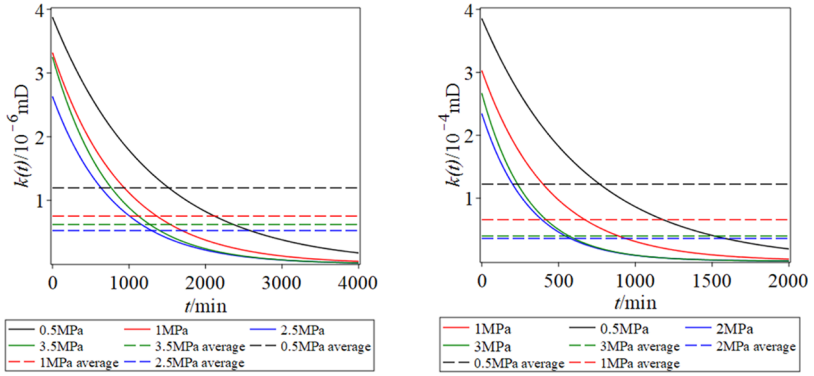

(a) granular coal (b) cylindrical coal

Figure 9. Decay of dynamic apparent permeability.

https://doi.org/10.1021/acsomega.3c03806
ACS Omega 2023, 8, 35964−35974

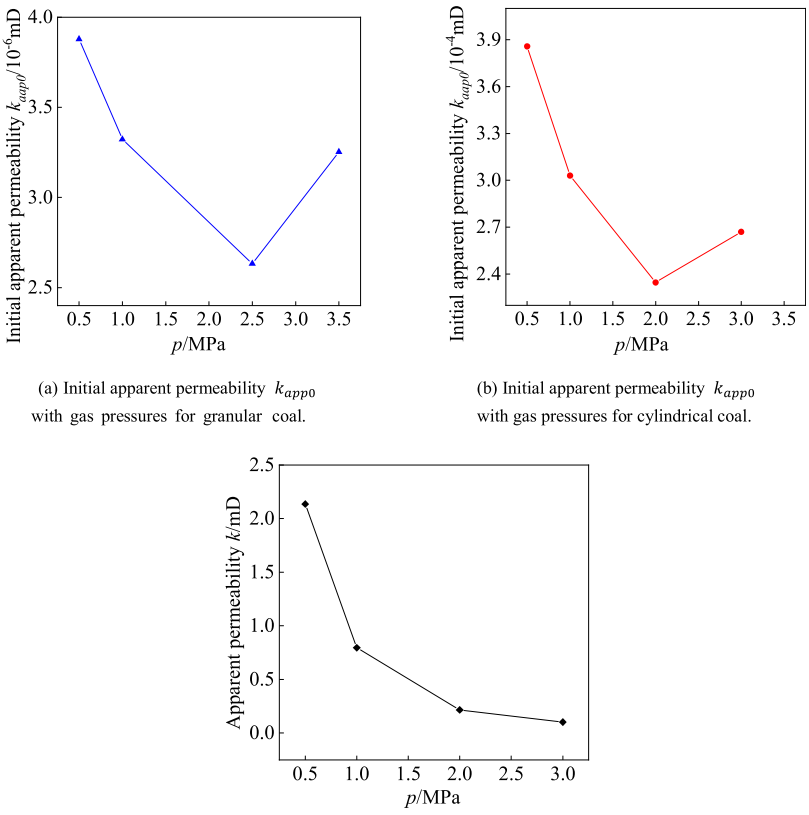

(a) Initial apparent permeability k_{app0} with gas pressures for granular coal.

(b) Initial apparent permeability k_{app0} with gas pressures for cylindrical coal.

(c) Steady-state apparent permeability k with gas pressures.

Figure 10. Change trend of permeability with the gas pressure.

$$k_{app} = k_{\infty 0}[1 + \alpha(Kn)Kn]\left[1 + \frac{4Kn}{1 + Kn}\right]$$
$$\frac{\phi}{\tau}\exp(-3c_t[(\bar{\sigma} - \bar{\sigma}_0) - (p - p_0)]) \quad (14)$$

where ϕ is the porosity, τ is the tortuosity, C_t is the compressibility of coal, $\bar{\sigma}$ is the average stress, $\bar{\sigma}_0$ is the initial average stress, p is the gas pressure, and p_0 is the initial gas pressure.

5.3. Influence Mechanism of Gas Pressure on Multi-scale Dynamic Apparent Diffusion-Permeability. The experimental data of the diffusion-seepage for granular and cylindrical coal are processed based on eq 11, and the attenuation of dynamic apparent permeability with time is plotted as follows.

As shown in Figure 9a,9b, the apparent dynamic permeability of the particle coal and cylindrical coal gradually decreases with time, presenting a dynamic decay trend. A crossover of the curves of dynamic apparent permeability occurs at different gas pressures. The dashed lines in Figure 9a,b are the average apparent permeability corresponding to the dynamic apparent permeability at each pressure, which are equivalent to the constant permeability converted by constant diffusion coefficient in eqs 2 and 4.

The apparent permeability at the beginning of the gas flow reflects the relationship between gas pressure and apparent permeability. Converting D_0, the initial apparent diffusion coefficient, into k_{app0}, the initial apparent permeability, the curves of k_{app0} with gas pressure for granular and cylindrical coal are shown in Figure 10a,10b. In addition, the apparent permeability measured by the steady-state method for cylindrical coal in Section 2 is presented in Figure 10c.

As shown in Figure 10a, the initial apparent permeability k_{app0} for granular coal shows a "U" shape with the increase of gas pressures and reaches the minimum value at 2.5 MPa of gas pressure. The permeability is divided into two stages by 2.5 MPa of gas pressure. At p < 2.5 MPa, k_{app0} decreases with increasing gas pressure; however, at p > 2.5 MPa, k_{app0} increases with increasing gas pressure. In Figure 10b, the variation of the initial apparent permeability with pressure for cylindrical coal is similar to that of granular coal in Figure 10a, showing a "U"-shaped change divided into two stages by 2 MPa of gas pressure.

The diffusion-seepage experiments for granular coal and columnar coal are conducted without stress loading. The comparison of Figure 10a, Figure 10b, and eq 14 revealed that the initial apparent permeability k_{app0} is affected by a combination of gas pressure expansion effect and slip effect.[30] The "U"-shaped change of initial apparent permeability with gas pressure depends on the contrasting relationship between the two effects. In Figure 10b, at p > 2.0 MPa, the apparent permeability for cylindrical coal is mainly influenced by the expansion effect of gas pressure. At this stage, the higher the gas pressure is, the higher the pressure difference is between the inside and outside of coal during diffusion-seepage. When the pressure difference exceeds the tensile strength of the coal, the pores in coal are stretched by the gas pressure difference.[31] At p < 2.0 MPa, the expansion effect of gas pressure in coal is weakened and the slip effect dominates with decreasing gas pressure. At this stage, the lower the gas pressure is, the more pronounced the slip effect is. In Figure 10a, the variational mechanism of gas pressure on the initial apparent permeability

https://doi.org/10.1021/acsomega.3c03806
ACS Omega 2023, 8, 35964−35974

for granular coal is similar to that of cylindrical coal in Figure 10b.

In Figure 10c, the apparent permeability, k, measured by the steady-state method for cylindrical coal under the effective stress decreases monotonically with the increase of gas pressure. The "U"-shaped variation does not appear, and the permeability decreases monotonically with the increase of gas pressure. The trend of monotonically decreasing appears. The reason is that the effective stress is larger under the stress loading, and a gas pressure of 3 MPa is not sufficient to crack the coal. The effect of gas expansion on the coal cannot expand the gas transport channel and the slip effect dominates, which cause the lower gas pressure, the more significant the slip effect, and the greater the permeability.

In eq 14, the Knudsen number, a measure of the flow regime, contains the variation of pore size and gas pressure. The pore structure of coal is multiscale; however, the micro- and nanopore sizes and gas pressures in coal cannot be observed during the experiment of diffusion-seepage. To simplify the analysis, the experimental data of cylindrical coal are selected to calculate the equivalent pore size of the initial apparent permeability at 0.5 MPa of gas pressure. According to eq 14, the impact mechanism of gas pressure on apparent permeability is investigated by changing the compressibility C_t of coal.

For C_t = 0.1 in Figure 11, the effect of the flow regime caused by gas pressure exceeds the gas expansion effect. The

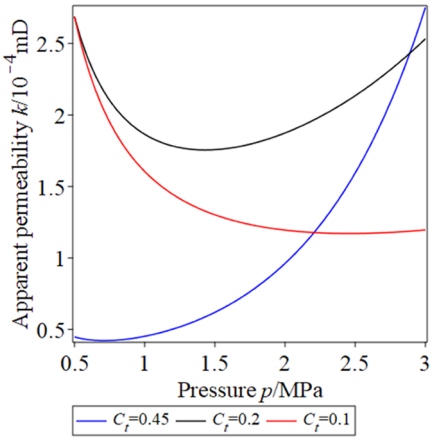

Figure 11. Effect of compressibility C_t on apparent permeability.

diffusion effect, including slip-transition-Knudsen diffusion, dominates the gas flow. Therefore, the apparent permeability shows a monotonic decrease with the increase of gas pressure. For C_t = 0.2, the effects of the flow regime and that of gas expansion are comparable, and the apparent permeability shows a "U"-shaped trend with gas pressure. For C_t = 0.45, the effect of gas expansion exceeds that of the flow regime and the apparent permeability shows a monotonic increase trend with increasing gas pressure. On the basis of eq 14 and Figure 11, it can be observed that the variation of apparent permeability with gas pressure is related to the compressibility of coal. The apparent permeability of coal with different compressibility will demonstrate monotonic decrease, monotonic increase, and "U"-shaped changes with increasing gas pressure, which depends on the contrasting relationship between the strength of the coal and the gas pressure. The main influence mechanism of gas pressure on multiscale permeability is the effect of gas expansion and flow regime.

6. RESULTS AND DISCUSSION

The low permeability of coal is a bottleneck problem that restricts the exploitation of coalbed methane, which has attracted widespread attention from the majority of scholars.[32−35] The results of the aforementioned studies show that permeability in coal presents two important new phenomena. (1) The permeability of gas flow in coal dynamically attenuates as time goes by. (2) During the gas extraction process, the change of permeability with the decrease of pressure presents three different results. Over the past decade, we have conducted at least 500 similar experiments, including granular coal, cylinder coal with or without stress loading, and covering most kinds of coal in China. We found that the two aforementioned laws of permeability change are generalizable and further discovered that the dynamic attenuation of the permeability is determined by the multiscale pores in the coal. Due to the reduction of pore size and gas pressure, it leads to different gas flow regimes in various different pore sizes, which further causes changes of gas permeability and flow mechanisms at different times. The above two results are important to further clarify the characteristics of the low permeability of coal and the influence of gas pressure on CBM extraction.

Our contributions are as follows in this paper. A novel model of radial multiscale dynamic permeability is proposed, which overcomes the defects of the constant coefficient model. Based on experimental comparisons, the new model is used to elucidate the mechanism of gas pressure on permeability.

7. CONCLUSIONS

(1) The classical diffusion model for cylindrical coal cannot accurately describe the full-time process of gas flow. A novel model of multiscale dynamic apparent diffusion-seepage is proposed to precisely depict the complete process of gas flow in coal. An expression of multiscale dynamic apparent permeability is derived based on the equivalent relationship between apparent diffusion coefficient and apparent permeability.

(2) Constrained by multiscale pores in coal, the process of gas diffusion-seepage presents a multiscale characteristic in space and time. In the early stage of flow, the gas flows out of the large pores first, in which the diffusion resistance is small and the apparent diffusion coefficient is large. As time goes by, from the surface to the inside, the apparent diffusion coefficient decreases and the diffusion resistance increases. The apparent diffusion coefficient shows a dynamic attenuation during the full-time process of gas diffusion-seepage.

(3) The gas flow in the coal is a continuous process of desorption, diffusion, and seepage. Depending on the pore size and gas pressure, the process of diffusion-seepage demonstrates various flow regimes such as continuous flow, slip flow, transition flow, and Knudsen diffusion flow. The expression of apparent permeability considering the impact of stress, gas pressure, and flow regime is established. The influence mechanism of gas pressure on the multiscale dynamic apparent diffusion-permeability is elucidated. The impact of the slip effect on apparent permeability is dominant at low gas

https://doi.org/10.1021/acsomega.3c03806
ACS Omega 2023, 8, 35964−35974

pressure, and that of gas expansion effect is dominant at high gas pressure. With increasing gas pressure, the apparent permeability present monotonic decrease, monotonic increase, and "U"-shaped changes, which is related to the gas pressures, the strength, and compressibility of coal C_t.

AUTHOR INFORMATION

Corresponding Author

Lin Li − *MOE Engineering Center of Mine Disaster Prevention and Rescue, Henan Polytechnic University, Jiaozuo, Henan 454000, China; Collaborative Innovation Center of Coal Work Safety and Clean High Efficiency Utilization, Henan Polytechnic University, Jiaozuo 454000, China; Collaborative Innovation Center of Coalbed Methane and Shale Gas for Central Plains Economic Region (Henan Province) and Henan Provincial Key Lab of Gas Geology and Control-Cultivation Base of Provincial and Ministry Joint State Key, Henan Polytechnic University, Jiaozuo, Henan 454000, China;* orcid.org/0009-0008-0232-8030; Email: 2780272737@qq.com

Authors

Zhiqiang Li − *MOE Engineering Center of Mine Disaster Prevention and Rescue, Henan Polytechnic University, Jiaozuo, Henan 454000, China; Collaborative Innovation Center of Coal Work Safety and Clean High Efficiency Utilization, Henan Polytechnic University, Jiaozuo 454000, China; Collaborative Innovation Center of Coalbed Methane and Shale Gas for Central Plains Economic Region (Henan Province) and Henan Provincial Key Lab of Gas Geology and Control-Cultivation Base of Provincial and Ministry Joint State Key, Henan Polytechnic University, Jiaozuo, Henan 454000, China*

Aijie Wang − *MOE Engineering Center of Mine Disaster Prevention and Rescue, Henan Polytechnic University, Jiaozuo, Henan 454000, China*

Junliang Li − *MOE Engineering Center of Mine Disaster Prevention and Rescue, Henan Polytechnic University, Jiaozuo, Henan 454000, China*

Ningchao Zhang − *MOE Engineering Center of Mine Disaster Prevention and Rescue, Henan Polytechnic University, Jiaozuo, Henan 454000, China*

Kaiqi Jin − *MOE Engineering Center of Mine Disaster Prevention and Rescue, Henan Polytechnic University, Jiaozuo, Henan 454000, China*

Ju Chang − *MOE Engineering Center of Mine Disaster Prevention and Rescue, Henan Polytechnic University, Jiaozuo, Henan 454000, China*

Complete contact information is available at: https://pubs.acs.org/10.1021/acsomega.3c03806

Notes

The authors declare no competing financial interest.

ACKNOWLEDGMENTS

This study was supported by the Fundamental Research Funds for the Universities of Henan Province (no. NSFRF180305) and the China Scholarship Council Fund (nos. 201808410203). This study was supported by the Doctoral Foundation of Henan Polytechnic University (B2021-7), the State Key Laboratory Cultivation Base for Gas Geology and Gas Control (Henan Polytechnic University) (no. WS2021A06), the Key Scientific Research Projects of Colleges and Universities in Henan Province (no. 22B620002), the Key Science and Technology Project of Henan Province (no. 222102320017).

REFERENCES

(1) Tan, Y.; Pan, Z.; Liu, J.; Kang, J.; Zhou, F.; Connell, L. D.; Yang, Y. Experimental study of impact of anisotropy and heterogeneity on gas flow in coal. Part I: Diffusion and adsorption. *Fuel* **2018**, *232*, 444−453.

(2) Tan, Y.; Pan, Z.; Liu, J.; Zhou, F.; Connell, L. D.; Sun, W.; Asadul, H. Experimental study of impact of anisotropy and heterogeneity on gas flow in coal. Part II: Permeability. *Fuel* **2018**, *230*, 397−409.

(3) Zhao, W.; Cheng, Y.; Pan, Z.; Wang, K.; Liu, S. Gas diffusion in coal particles: A review of mathematical models and their applications. *Fuel* **2019**, *252*, 77−100.

(4) Sander, R.; Pan, Z.; Connell, L. D. Laboratory measurement of low permeability unconventional gas reservoir rocks: A review of experimental methods. *J. Nat. Gas Sci. Eng.* **2017**, *37*, 248−279.

(5) Pan, Z.; Connell, L. D. Modelling permeability for coal reservoirs: A review of analytical models and testing data. *Int. J. Coal Geol.* **2012**, *92*, 1−44.

(6) Xu, H.; Tang, D.; Zhao, J.; Li, S.; Shu, T. A new laboratory method for accurate measurement of the methane diffusion coefficient and its influencing factors in the coal matrix. *Fuel* **2015**, *158*, 239−247.

(7) Yi, M.; Wang, L.; Cheng, Y.; Wang, C.; Hu, B. Calculation of gas concentration-dependent diffusion coefficient in coal particles: Influencing mechanism of gas pressure and desorption time on diffusion behavior. *Fuel* **2022**, *320*, No. 123973.

(8) Yan, J.; Meng, Z.; Li, G. Diffusion characteristics of methane in various rank coals and the control mechanism. *Fuel* **2021**, *283*, No. 118959.

(9) Wang, L.; Zhang, G.; Liu, J.; Chen, X.; Li, Z. Effect of the Pore Structure on Adsorption and Diffusion Migration of Different Rank Coal Samples. *Energy Fuels.* **2020**, *34*, 12486−12504.

(10) Meng, Y.; Li, Z. Experimental study on diffusion property of methane gas in coal and its influencing factors. *Fuel* **2016**, *185*, 219−228.

(11) Du, Y.; Chen, X.; Li, L.; Wang, P. Characteristics of methane desorption and diffusion in coal within a negative pressure environment. *Fuel* **2018**, *217*, 111−121.

(12) Staib, G.; Richard, S.; Evan Mac A, G. Dispersive diffusion of gases in coals. Part II: An assessment of previously proposed physical mechanisms of diffusion in coal. *Fuel* **2015**, *143*, 620−629.

(13) Pillalamarry, M.; Harpalani, S.; Liu, S. Gas diffusion behavior of coal and its impact on production from coalbed methane reservoirs. *Int. J. Coal Geol.* **2011**, *86*, 342−348.

(14) Liu, A.; Liu, P.; Liu, S. Gas diffusion coefficient estimation of coal: A dimensionless numerical method and its experimental validation. *Int. J. Heat Mass Transfer* **2020**, *162*, No. 120336.

(15) Liu, Z.; Cheng, Y.; Dong, J.; Jiang, J.; Wang, L.; Li, W. Master role conversion between diffusion and seepage on coalbed methane production: Implications for adjusting suction pressure on extraction borehole. *Fuel* **2018**, *223*, 373−384.

(16) Yang, Y.; Liu, S. Integrated modeling of multi-scale transport in coal and its application for coalbed methane recovery. *Fuel* **2021**, *300*, No. 120971.

(17) Wang, Y.; Liu, S. Estimation of pressure-dependent diffusive permeability of coal using methane diffusion coefficient: laboratory measurements and modeling. *Energy Fuels* **2016**, *30*, 8968−8976.

(18) Kang, J.; Zhang, B.; Kang, T. Monte Carlo and molecular dynamic simulations of CH_4 diffusion in kaolinite as functions of pressure and temperature. *J. Nat. Gas Sci. Eng.* **2018**, *54*, 65−71.

(19) Yang, X.; Wang, G.; Zhang, J.; Ren, T. The Influence of sorption pressure on gas diffusion in coal particles: an experimental study. *Processes* **2019**, *7*, No. 219.
(20) Yang, X.; Zhang, J.; Wang, G.; Ren, T. Experimental study of the influence of gas pressure on the gas diffusion in coal. *J. China Univ. Min. Technol.* **2019b**, *483*, 503−519.
(21) Li, X.; Li, Z.; Ren, T.; Nie, B.; Xie, L.; Huang, T.; Bai, S.; Jiang, Y. Effects of particle size and adsorption pressure on methane gas desorption and diffusion in coal. *Arabian J. Geosci.* **2019**, *12*, No. 794.
(22) Li, Z.; Liu, D.; Cai, Y.; Shi, Y. Investigation of methane diffusion in low-rank coals by a multiparous diffusion model. *J. Nat. Gas Sci. Eng.* **2016b**, *33*, 97−107.
(23) Li, Z.; Wang, D.; Song, D. Influence of temperature on dynamic diffusion coefficient of CH_4 into coal particles by new diffusion model. *J. China Coal Soc.* **2015**, *40* (5), 1055−1064.
(24) Yang, Y.; Liu, S. Estimation and modeling of pressure-dependent gas diffusion coefficient for coal: A fractal theory-based approach. *Fuel* **2019**, *253*, 588−606.
(25) Pone, J. D. N.; Halleck, P. M.; Mathews, J. P. Sorption capacity and sorption kinetic measurements of CO2 and CH4 in confined and unconfined bituminous coal. *Energy Fuels* **2009**, *23*, 4688−4695.
(26) Crank, J. *The Mathematic of Diffusion*, 2nd ed.; Oxford University Press: Oxford, 1975.
(27) Li, Z.; Peng, J.; Li, L.; Qi, L.; Li, W. Novel dynamic multiscale Model of apparent diffusion permeability of methane through low-permeability coal seams. *Energy Fuels* **2021**, *35*, 7844−7857.
(28) Ziarani, A. S.; Aguilera, R. Knudsen's permeability correction for tight porous media. *Transp Porous Med.* **2012**, *91*, 239−260.
(29) Cao, P.; Liu, J.; Leong, Y.-K. Combined impact of flow regimes and effective stress on the evolution of shale apparent permeability. *J. Unconv. Oil Gas Resour.* **2016**, *14*, 32−43.
(30) Klinkenberg, L. J. The Permeability of Porous Media to Liquids and Gases. In *Proceedings of Drilling and Production Practice*; American Petroleum Institute: New York, 1941; pp 200−213.
(31) Wang, S.; Elsworth, D.; Liu, J. Rapid decompression and desorption induced energetic failure in coal. *J. Rock Mech. Geotech. Eng.* **2015**, *7*, 345−350.
(32) Tao, S.; Chen, S.; Pan, Z. Current status, challenges, and policy suggestions for coalbed methane industry development in China: A review. *Energy Sci. Eng.* **2019**, *7*, 1059−1074.
(33) Tao, S.; Pan, Z.; Tang, S.; Chen, S. Current status and geological conditions for the applicability of CBM drilling technologies in China: A review. *Int. J. Coal Geol.* **2019**, *202*, 95−108.
(34) Tao, S.; Tang, D.; Xu, H.; Li, S.; Geng, J.; Zhao, J.; Wu, S.; Meng, Q.; Kou, X.; Yang, S.; Yi, C. Fluid velocity sensitivity of coal reservoir and its effect on coalbed methane well productivity: A case of Baode Block, northeastern Ordos Basin, China. *J. Pet. Sci. Eng.* **2017**, *152*, 229−237.
(35) Men, X.; Tao, S.; Liu, Z.; Tian, W.; Chen, S. Experimental study on gas mass transfer process in a heterogeneous coal reservoir. *Fuel Process. Technol.* **2021**, *216*, No. 106779.

https://doi.org/10.1021/acsomega.3c03806
ACS Omega 2023, 8, 35964−35974